

Surface-normal electro-optic-polymer modulator with silicon subwavelength grating

Yuji Kosugi^{1a)}, Toshiki Yamada², Akira Otomo²,
Yoshiaki Nakano¹, and Takuo Tanemura¹

¹ Department of Electrical Engineering and Information Systems,
School of Engineering, The University of Tokyo,
7-3-1 Hongo, Bunkyo-ku, Tokyo 113-8656, Japan

² National Institute of Information and Communications Technology,
588-2 Iwaoka, Nishi-ku, Kobe 651-2492, Japan

a) kosugi@hotaka.t.u-tokyo.ac.jp

Abstract: We propose novel silicon-based surface-normal optical modulator using electro-optic (EO) polymer. The EO polymer is embedded inside a thin silicon subwavelength grating layer, which is used as both the interdigitated electrodes for effective poling of the EO polymer, and as high-Q resonant structure for the incident light to enable efficient modulation. We numerically demonstrate 10-dB intensity modulation at 1550-nm wavelength under a refractive index change of only 3.8×10^{-4} , corresponding to the driving voltage below 1 V. Total-reflectance phase modulator is also demonstrated by adding a backside reflector. With inherently high-speed response over several tens of GHz, scalability to dense 2-D array integrated with CMOS driver circuitry, and relatively easy and low-cost fabrication without epitaxial process, the proposed device may find versatile applications in optical interconnects, free-space optical communications, imaging and sensing.

Keywords: surface-normal modulator, spatial light modulator, electro-optic polymer, high-contrast grating

Classification: Integrated optoelectronics

References

- [1] A. Kirk, *et al.*: “Design and implementation of a modulator-based free-space optical backplane for multiprocessor applications,” *Appl. Opt.* **42** (2003) 2465 (DOI: [10.1364/AO.42.002465](https://doi.org/10.1364/AO.42.002465)).
- [2] R. M. Audet, *et al.*: “Surface-normal Ge/SiGe asymmetric Fabry–Perot optical modulators fabricated on silicon substrates,” *J. Lightwave Technol.* **31** (2013) 3995 (DOI: [10.1109/JLT.2013.2279174](https://doi.org/10.1109/JLT.2013.2279174)).
- [3] W. S. Rabinovich, *et al.*: “Free-space optical communications research and demonstrations at the U.S. naval research laboratory,” *Appl. Opt.* **54** (2015) F189 (DOI: [10.1364/AO.54.00F189](https://doi.org/10.1364/AO.54.00F189)).
- [4] A. P. Mosk, *et al.*: “Controlling waves in space and time for imaging and

- focusing in complex media,” *Nat. Photonics* **6** (2012) 283 (DOI: [10.1038/nphoton.2012.88](https://doi.org/10.1038/nphoton.2012.88)).
- [5] C. Maurer, *et al.*: “Tailoring of arbitrary optical vector beams,” *New J. Phys.* **9** (2007) 78 (DOI: [10.1088/1367-2630/9/3/078](https://doi.org/10.1088/1367-2630/9/3/078)).
- [6] W. Yang, *et al.*: “High speed optical phased array using high contrast grating all-pass filters,” *Opt. Express* **22** (2014) 20038 (DOI: [10.1364/OE.22.020038](https://doi.org/10.1364/OE.22.020038)).
- [7] Y. Kanamori, *et al.*: “Fabrication of transmission color filters using silicon subwavelength gratings on quartz substrates,” *IEEE Photon. Technol. Lett.* **18** (2006) 2126 (DOI: [10.1109/LPT.2006.883208](https://doi.org/10.1109/LPT.2006.883208)).
- [8] C. J. Chang-Hasnain and W. Yang: “High contrast gratings for integrated optoelectronics,” *Adv. Opt. Photonics* **4** (2012) 379 (DOI: [10.1364/AOP.4.000379](https://doi.org/10.1364/AOP.4.000379)).
- [9] L. R. Dalton, *et al.*: “Electric field poled organic electro-optic materials: State of the art and future prospects,” *Chem. Rev.* **110** (2010) 25 (DOI: [10.1021/cr9000429](https://doi.org/10.1021/cr9000429)).
- [10] X. Piao, *et al.*: “Nonlinear optical side-chain polymers post-functionalized with high- β chromophores exhibiting large electro-optic property,” *J. Polym. Sci. A Polym. Chem.* **49** (2011) 47 (DOI: [10.1002/pola.24410](https://doi.org/10.1002/pola.24410)).
- [11] T. Yamada and A. Otomo: “Usefulness of transmission ellipsometric method for evaluation of electro-optic materials,” *IEICE Trans. Electron.* **E98-C** (2015) 143 (DOI: [10.1587/transele.E98.C.143](https://doi.org/10.1587/transele.E98.C.143)).
- [12] R. Palmer, *et al.*: “High-speed, low drive-voltage silicon-organic hybrid modulator based on a binary-chromophore electro-optic material,” *J. Light-wave Technol.* **32** (2014) 2726 (DOI: [10.1109/JLT.2014.2321498](https://doi.org/10.1109/JLT.2014.2321498)).
- [13] Y. Horie, *et al.*: “Guided resonance reflective phase shifters,” *Proc. SPIE* **9372** (2015) 93720W (DOI: [10.1117/12.2077744](https://doi.org/10.1117/12.2077744)).
- [14] High Contrast Grating Solver Package, Univ. of California, Berkeley: <https://light.eecs.berkeley.edu/cch/hcgsolver.html>.

1 Introduction

Surface-normal integrated optical modulators that operate on optical beams oriented perpendicular to the chip surface rather than in-plane waveguide configuration have attracted considerable attention in diverse field of optics. Having inherent compatibility with dense 2-D array integration, they have found wide range of potential applications, including high-capacity optical interconnects [1, 2], free-space optical communications [3], dynamic beam forming and adaptive optics [4, 5]. Surface-normal modulators based on liquid crystals and micro-electro-mechanical systems (MEMS) are relatively mature; but their operating speed is typically in a range from kHz up to MHz [4, 5, 6]. On the other hand, high-speed surface-normal intensity modulators with bandwidth beyond GHz range have been demonstrated by using multiple-quantum-well (MQW) semiconductor materials [1, 2, 3]. These devices, however, require complicated epitaxial structures and are inherently absorptive, which makes them unsuitable for some applications.

In this paper, we propose a novel silicon-based surface-normal optical modulator using electro-optic (EO) polymer. By embedding EO polymer inside 856-nm-thick silicon (Si) subwavelength high-contrast grating (HCG) layer, we numerically demonstrate efficient intensity and phase modulation at 1550-nm wavelength with a required driving voltage below 1 V. Owing to the high-speed Pockels effect of

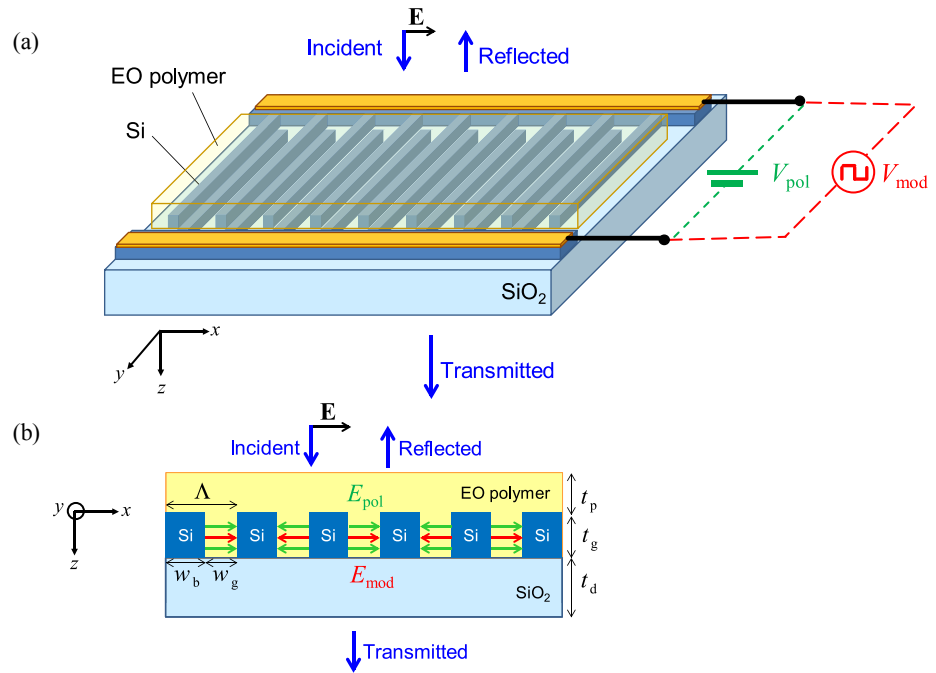


Fig. 1. (a) Schematic illustration of the surface-normal modulator using EO polymer embedded inside silicon subwavelength grating. (b) Cross-sectional view of the device structure with the definitions of geometric parameters.

the EO polymer, they can potentially be operated at several tens of GHz or faster with the modulation bandwidth only limited by the RC constant. Moreover, the proposed modulator can be readily scaled to a dense 2-D array with integrated CMOS driver circuitry, making it attractive for optical interconnects and imaging applications.

2 Proposed surface-normal modulator: Structure and principle

The schematic of the proposed optical modulator is depicted in Fig. 1. It consists of a thin (typically less than $1\ \mu\text{m}$) Si subwavelength grating formed on top of a dielectric (SiO₂) layer. By setting the period of grating Λ to be shorter than the wavelength of light, diffraction of incident light is prohibited. Moreover, due to the large contrast in refractive index between the Si grating and surrounding materials, it works as HCG, which can, with a careful design of geometrical parameters, operate either as a high-Q resonator or broadband reflector [6, 7, 8].

In order to achieve electro-optic tuning of the resonant property, we coat the entire grating with EO polymer [9, 10, 11, 12]. The Si grating layer is patterned in a comb shape as shown in Fig. 1 and lowly doped so that it can be used as interdigitated electrodes for applying the poling voltage V_{pol} . During the poling process, therefore, EO polymer is periodically poled as shown by the green arrows (E_{pol}) in Fig. 1, inducing an electro-optic coefficient r_{33} with opposite signs inside the adjacent gaps. Here, note that “3” in r_{33} corresponds to the x axis of the coordinate shown in Fig. 1.

The refractive index of the EO polymer for transverse-magnetic (TM) light (having electric field oriented perpendicular to the grating as shown in Fig. 1) can

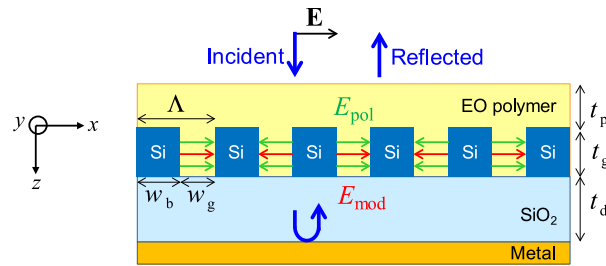


Fig. 2. The structure of total-reflectance high-speed phase modulator with a metallic reflector.

then be modulated via the Pockels effect by applying a modulating voltage V_{mod} . The change in refractive index is expressed as

$$\Delta n = -\frac{1}{2}n_0^3r_{33}E_{\text{mod}}, \quad (1)$$

where n_0 is the refractive index of the EO polymer without modulation and E_{mod} ($= V_{\text{mod}}/w_g$, with w_g being the width of the grating gap) is the modulating electric field along the x -axis. By using the same interdigitated Si electrodes for modulation, we can apply electric field E_{mod} as shown by red arrows in Fig. 1. Since the factor $r_{33}E_{\text{mod}}$ in Eq. (1) has identical sign and magnitude inside all gaps, the refractive index of EO polymer between the grating bars changes uniformly upon modulation. As a result, we can modify the resonant property of HCG and modulate both the reflectance and transmittance of TM-polarized light near the resonant wavelength. Since the change of refractive index of EO polymer originates from electronic polarization, we can achieve inherently high-speed modulation [12], with the bandwidth only limited by the RC delay of the Si electrodes.

While the device shown in Fig. 1 operates as an intensity modulator, we can also realize a total-reflectance high-speed phase modulator by adding a metallic mirror with nearly perfect reflectivity as shown in Fig. 2 [13]. When the optical absorption inside the HCG is negligible, we can modulate only the phase of the reflected light without changing its intensity. With dense 2-D array integration, such a device should be useful in dynamic beam shaping and adaptive optics, with the operating speed much faster than that of conventional spatial light modulators [4, 5].

3 Numerical results

The transmittance and reflectance characteristics of the proposed device are calculated for TM-polarized light by using the eigenmode-expansion-based analytical method [8, 14]. Assuming 1550-nm wavelength range, we set the refractive indices of Si and SiO₂ to be $n_{\text{Si}} = 3.48$ and $n_{\text{SiO}_2} = 1.44$, respectively. We assume the refractive index of EO polymer before applying modulation to be $n_0 = 1.60$.

3.1 Surface-normal intensity modulator

We first analyze the reflectance property of the device shown in Fig. 1 without modulation. For simplicity, we consider a case of $w_b = w_g$, where w_b and w_g are the width of the Si grating bars and the gaps between them, respectively. We also

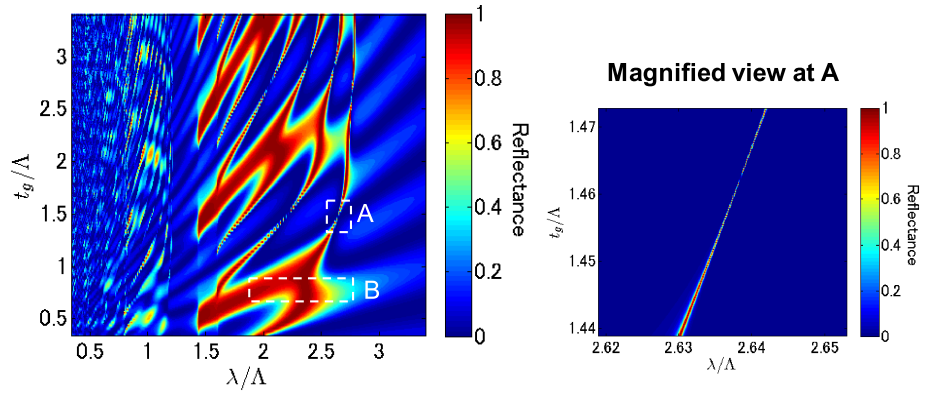


Fig. 3. The relationship between the thickness t_g of the grating and the reflectivity spectrum when $w_b = w_g$. The maker A and B indicate the regimes where HCG works as high-Q resonator and broadband reflector, respectively. The enlarged view of the plot near regime A is shown in the inset.

assume the thicknesses of the top EO polymer and bottom SiO₂ layers, t_p and t_d , to be infinite. Such assumption is equivalent to the case where we have ideal anti-reflection coating on the both sides.

Fig. 3 shows the calculated spectral property of reflectance as a function of normalized grating thickness t_g/Λ and wavelength λ/Λ , where Λ is the grating period, t_g is the thickness of the Si grating layer, and λ is the wavelength. Note that Fig. 3 only depends on the normalized thickness and wavelength, and remains valid at arbitrary wavelength range as long as we scale each dimension accordingly. When $\lambda/\Lambda > n_{\text{SiO}_2}$, the grating period becomes subwavelength, so that diffraction is suppressed. In particular, when λ/Λ is in the range from 1.44 to around 2.83, a characteristic checkerboard-like pattern emerges in Fig. 3 as a result of optical interference between two guiding modes inside the HCG layer [8]. We see from Fig. 3 that depending on t_g/Λ , HCG operates as a high-Q resonator (for example, regime A in Fig. 3) or a reflective mirror with broad spectral bandwidth (regime B in Fig. 3).

By using the high-Q resonator regime, we can demonstrate surface-normal intensity modulator. For this purpose, regime A in Fig. 3 is selected because t_g is smallest among other high-Q resonant conditions, alleviating the fabrication difficulty to embed EO polymer inside the grating gaps. By setting the resonance wavelength to be 1550 nm, other parameters are determined automatically from Fig. 3 as $\Lambda = 588$ nm, $w_b = w_g = \Lambda/2 = 294$ nm, and $t_g = 856$ nm. We assume that the refractive index of EO polymer is modulated uniformly only inside the regions between Si bars as we apply the modulation voltage V_{mod} .

Fig. 4(a) shows the calculated reflectance for various values of n_{EO} . We see a sharp resonant peak with a Q factor larger than 50,000. The resonant wavelength shifts continuously from 1549.2 nm to 1550.9 nm as n_{EO} changes from 1.59 to 1.61. As an example case, if we fix the signal wavelength to 1550 nm, the intensity of reflected light can be modulated by varying n_{EO} as shown in Fig. 4(b). We see that 10-dB intensity modulation can be obtained with Δn of only 3.8×10^{-4} . Inserting $\Delta n = 3.8 \times 10^{-4}$ and $w_g = 294$ nm to Eq. (1) and assuming a typical thermally

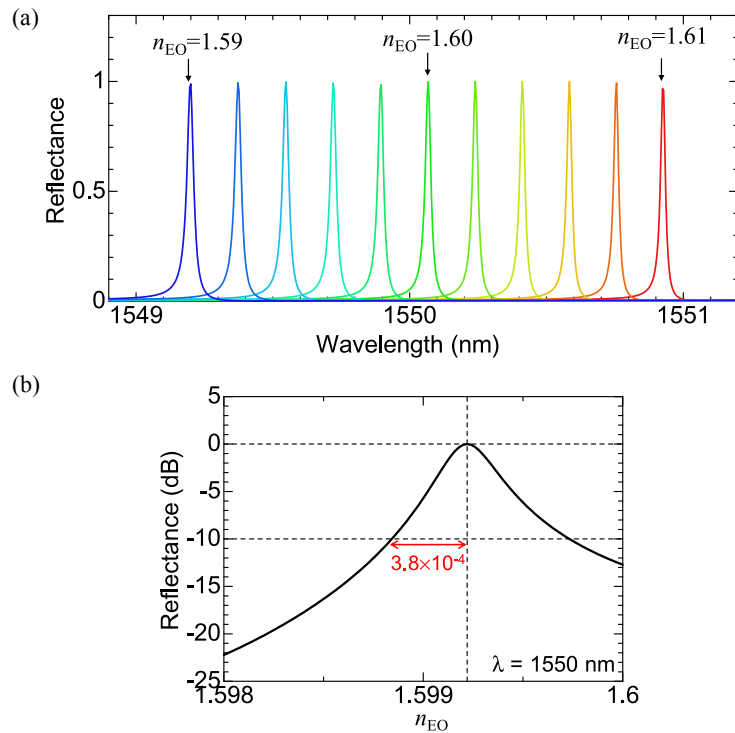


Fig. 4. (a) Reflectance characteristic with n_{EO} varied from 1.59 to 1.61 with a step of 0.002. (b) Intensity modulation characteristic of reflected light at 1550 nm (TM mode, $\Lambda = 588$ nm, $w_b = w_g = 294$ nm, $t_g = 856$ nm).

stable EO polymer with $r_{33} = 100$ pm/V [9, 10, 11], we estimate that the required driving voltage can be as small as $V_{mod} = \pm 0.27$ V. Moreover, if we could employ more recent EO polymers with enhanced r_{33} exceeding 200 pm/V [12], the driving voltage could be reduced further. Depending on application, we could also modulate the intensity of the transmitted light. The modulation property of the transmitted light is complementary to that shown in Fig. 4.

3.2 Total-reflectance phase modulator

As discussed in Section 2, we can also realize all-pass phase modulator by adding a highly reflective mirror as shown in Fig. 2. Similar to the case in Fig. 4, we assume $\Lambda = 588$ nm, $w_b = w_g = 294$ nm, and $t_g = 856$ nm, while we set the SiO₂ layer thickness to be $t_d = 800$ nm and we assume a silver mirror with the complex refractive index of $n_{metal} = 0.469 - 9.320i$.

The intensity and phase characteristics of the reflected light are shown in Fig. 5(a). We see that the optical phase of reflected light changes sharply near the resonance wavelength, while its intensity is kept almost constant with the reflectivity above 0.97. When the resonant wavelength is modulated by applying voltage V_{mod} , efficient phase modulation is obtained at 1550-nm wavelength as shown in Fig. 5(b). Required refractive index modulation to achieve π shift is $\Delta n = 5.4 \times 10^{-4}$, which correspond to $V_{mod} = \pm 0.39$ V if we assume $r_{33} = 100$ pm/V. With dense 2-D array integration capability, the demonstrated phase modulator should be useful in high-speed beam shaping and adaptive optics.

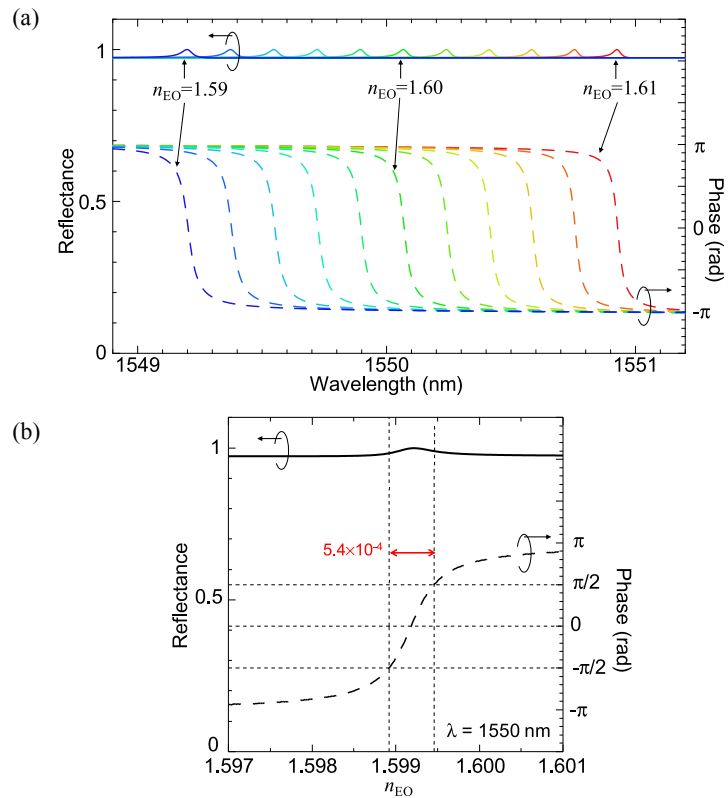


Fig. 5. (a) The intensity and phase characteristics of the reflected light with n_{EO} varied from 1.59 to 1.61 with a step of 0.002. (b) Intensity and phase modulation characteristic of reflected light at 1550 nm (TM mode, $\Lambda = 588$ nm, $w_b = w_g = 294$ nm, $t_g = 856$ nm).

4 Wavelength tunability by tilting incident angle

While efficient intensity/phase modulation is possible by the proposed surface-normal modulator, such modulation is obtained only at the resonant wavelength of HCG, which severely limits the operating wavelength range of the device. To solve this constraint, we demonstrate here that the resonant wavelength could be precisely tuned by adjusting the incident angle of light.

Fig. 6(a) shows the schematic of the device used under tilted incident light having a wave vector of (k_x, k_y, k_z) . When the incident light is tilted by an angle φ within yz -plane, k_y becomes nonzero and k_z decreases to $k_z = \sqrt{k_0^2 - k_y^2}$, where k_0 is the wave number. In this case, we obtain essentially similar resonant property of HCG (since $k_x = 0$), whereas the equivalent thickness t_g decreases due to reduced k_z . As a result, we see from Fig. 3 that we can tune the resonant wavelength by adjusting φ .

Fig. 7 shows how the resonant wavelength changes as we increase the incident angle φ . We see that the operating wavelength of the modulator can be tuned over 30 nm (1520–1550 nm) with an incident angle range of only 18.6 deg. In practice, incident angle can be adjusted by simply rotating the device as shown in Fig. 6(b) for the transmitting configuration, or by shifting the position of the input and output port at the Fourier plane as shown in Fig. 6(c) for the reflecting configuration.

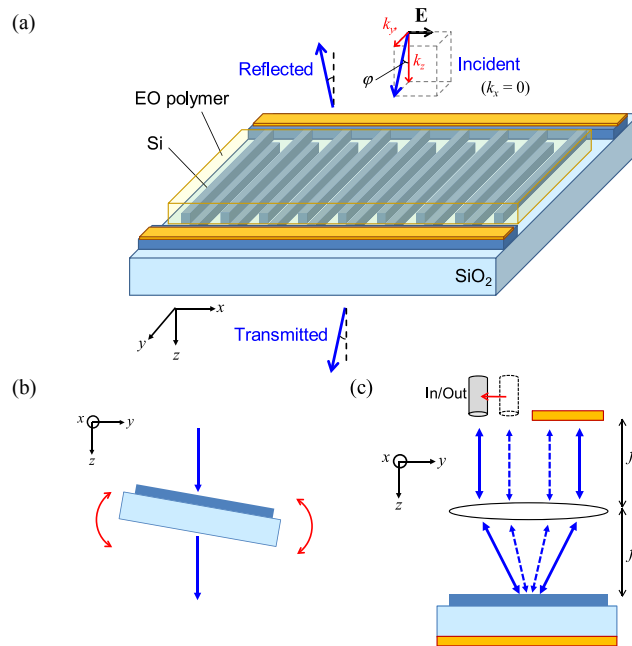


Fig. 6. (a) Schematic of the device used under a tilted incident angle for wavelength tuning. (b, c) Practical tuning schemes that could be employed in either transmitting (b) and reflecting (c) configurations.

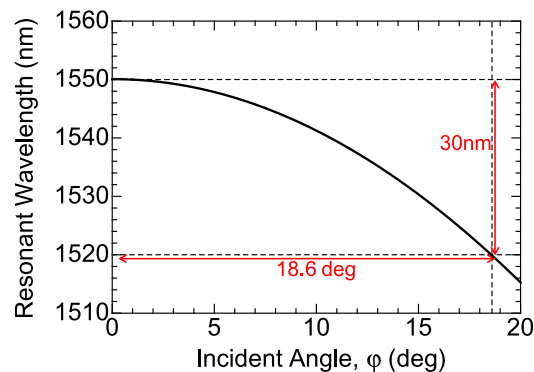


Fig. 7. Resonant wavelength with increasing incident angle (TM mode, $\Lambda = 588$ nm, $w_b = w_g = 294$ nm, $t_g = 856$ nm)

5 Conclusion

We have proposed and numerically demonstrated a novel type of surface-normal optical modulator using a thin ($< 1 \mu\text{m}$) silicon subwavelength grating coated with EO polymer. The silicon grating was employed for two purposes: (1) to induce resonant guided modes for the incident light and (2) to periodically pole the EO polymer with opposite sign inside the adjacent gaps. With a refractive index modulation of less than 10^{-3} applied to the EO polymer inside the gaps, we numerically demonstrated efficient intensity modulation with extinction ratio over 10 dB as well as total-reflectance phase modulator, both at 1550-nm wavelength. Assuming a typically available EO polymer with $r_{33} = 100$ pm/V, we estimate that the driving voltage for modulation to be below 1 V. Finally, the operating wavelength could be tuned precisely by adjusting the incident angle of light, which

would greatly enhance the practicability of the device. With inherently high-speed modulation response over several tens of GHz, potential scalability to dense 2-D array integrated with CMOS driver circuitry, and relatively easy and low-cost fabrication without epitaxial process, the proposed devices may be useful in wide ranges of applications, including optical interconnects, free-space optical communications, and high-speed optical beam shaping for imaging and sensing.